

5-17-1993

BCG Cell Imaging Using Scanning Probe Microscopy

Antonio A. Garcia
Arizona State University

William C. Pettigrew
Arizona State University

John Graham
Park Scientific Co.

Follow this and additional works at: <https://digitalcommons.usu.edu/microscopy>



Part of the [Biology Commons](#)

Recommended Citation

Garcia, Antonio A.; Pettigrew, William C.; and Graham, John (1993) "BCG Cell Imaging Using Scanning Probe Microscopy," *Scanning Microscopy*: Vol. 7 : No. 2 , Article 14.

Available at: <https://digitalcommons.usu.edu/microscopy/vol7/iss2/14>

This Article is brought to you for free and open access by the Western Dairy Center at DigitalCommons@USU. It has been accepted for inclusion in Scanning Microscopy by an authorized administrator of DigitalCommons@USU. For more information, please contact digitalcommons@usu.edu.



BCG CELL IMAGING USING SCANNING PROBE MICROSCOPY

Antonio A. Garcia*, William C. Pettigrew, and John Graham¹

Department of Chemical, Biological, and Materials Engineering
Arizona State University, Tempe, AZ 85287-6006

¹Park Scientific Co., 1171 Boregas Avenue, Sunnyvale, California 94089

(Received for publication May 12, 1992, and in revised form May 17, 1993)

Abstract

Scanning tunneling microscopy (STM) and atomic force microscopy (AFM) were used to obtain images of the surface of whole, intact BCG (bacille Calmette Guerin, a mycobacterium) cells in air and under solution by immobilizing the cells onto glass slides (AFM only) or highly oriented pyrolytic graphite. The technique used for AFM imaging involved depositing a submonolayer of cells under a centrifugal force followed by fixation/dehydration using polar organic solvents. AFM images agree well with images from light and electron microscopy and showed large numbers of BCG cells in their distinctive cord arrangement. The AFM also proved useful for identifying extracellular microgranules which cannot be seen with light microscopy.

For STM imaging, the hydrophobicity of BCG enabled strong adhesion from aqueous solution onto graphite. STM images of BCG could only be obtained while scanning in aqueous solution, and the cells showed a large variation in contrast when different samples were imaged. The STM provided greater detail of surface features than the AFM and was able to produce images of periodic layers corroborating observations made by transmission electron microscopy.

KEY WORDS: Atomic force microscope, scanning tunneling microscope, scanning probe microscope, bacille Calmette-Guerin, BCG, vaccine adjuvants, imaging, BCG cords, cell.

*Address for Correspondence:

Antonio A. Garcia
Department of Chem., Bio., and Matls. Eng.,
Arizona State University,
Tempe, AZ 85287-6006

Phone: (602) 965-8798
FAX: (602) 965-8296

Introduction

Scanning probe microscopes (SPM) such as the scanning tunneling microscopes (STM) and the atomic force (AFM) microscopes are relatively new instruments capable of studying the topography of surfaces and adsorbates in vacuum, air, or under solution. Although recent advances in other microscopies have resulted in improved image resolution of biological specimens with these more established techniques, SPM can provide information on biological materials under aqueous solution. In fact, SPM hold promise as a tool for understanding detailed surface morphology of biopolymers and cells under a variety of environments. However, in order to conduct meaningful studies of a particular cell or micron-scale biological material with scanning probe instruments, sample immobilization procedures (preferably techniques which do not involve stains or coats that obliterate fine surface features) must first be well established.

Several techniques have been used to image whole cells with the scanning force microscope. Halobacteria were imaged with the AFM by spreading the cells onto a glass slide and allowing them to dry (Butt *et al.*, 1990). Haberle *et al.* (1991) were the first to image immunogold labelled cells in an aqueous solution by sucking the cells with a microcapillary. This pipet technique was also used to study monkey culture cells and human erythrocytes in buffered solution for long periods of time (Hörber *et al.*, 1992). Putnam *et al.* (1992) imaged T-lymphocytes in air by preparing cyto centrifuge slides and fixing the cells with formaldehyde and acetone. Chemical immobilization using polylysine (Hörber *et al.*, 1992; Butt *et al.*, 1990; Gould *et al.*, 1990) and 3-aminopropyltriethoxysilane (Butt *et al.*, 1990) or immobilization of cells using protein tethers such as collagen or mixtures of extractin, collagen, and laminin (Henderson *et al.*, 1992) as well as the natural adhesion processes that cells induce when cultured on glass (Kasa *et al.*, 1993) have also been demonstrated.

Cell imaging with the STM has been performed under aqueous solution and in air. Chinese hamster ovary fibroblast and a human bladder cancer cell were imaged under aqueous solution by allowing them to

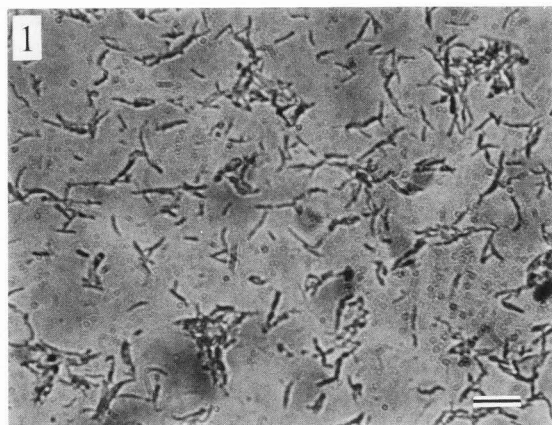


Figure 1. An optical microscope image of BCG cells immobilized on a glass slide. Bar = 10 μm .

culture on a highly oriented pyrolytic graphite (HOPG) substrate (Ito *et al.*, 1991). Ruppertsberg *et al.* (1989) also used HOPG to image human medulloblastoma cells and oocytes from a toad using the STM in air.

The smaller number of cell studies with STM as compared with AFM is likely due to the lack of understanding of how insulating materials can be imaged which makes the task of image interpretation a daunting one. However, recent work by Tang *et al.* (1993) suggests that molecular resolution of thick (hundreds of angstroms) insulators with the STM is possible through a non-tunneling mechanism. Two observations to be noted from this work are: (1) small changes in bias voltage causing the STM to penetrate the cellulose sample; and (2) large tunneling current fluctuations which were also reported by the researchers imaging cells with the STM. If this non-tunneling mechanism can be utilized for imaging uncoated cells, the potential exists for improving scanning probe microscopy resolution from the currently attainable AFM resolution of 10 nm (Hörber *et al.*, 1992).

Tuberculosis is still the leading cause of death in the world. *Mycobacterium tuberculosis* and *Mycobacterium lepra*, which causes leprosy, are pathogenic organisms that are examples of the group known as the mycobacteria. The success of bacille Calmette-Guerin (BCG cells) as a vaccine against tuberculosis led to its widespread use (Smith, 1984). It has also been realized that BCG can be effective as a vaccine adjuvant (Stewart-Tull, 1983) or in a similar vein as a multivaccine vehicle by growing rBCG (Stover *et al.*, 1991).

The initial goal of our research is to develop techniques using scanning probe microscopes to study the detailed morphology of vaccine adjuvants. After scanning and sample preparation techniques are well established, the next hurdle is to determine how to interpret imaging results since image convolution due to probe geometry and probe induced forces could create artifacts. We chose to do the initial imaging work with BCG and

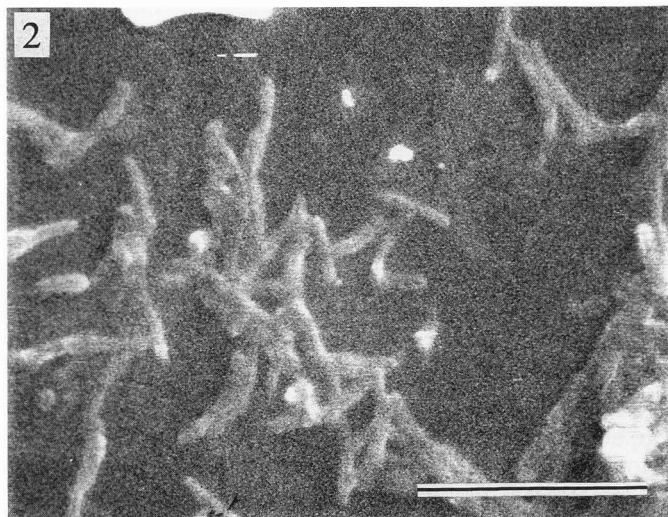


Figure 2. Scanning electron microscope image of BCG cells immobilized on a glass slide and coated with aluminum. Bar = 10 μm .

a particle derived from the cell wall of *Saccharomyces cerevisiae* with the trade name of Adjuvax[®] [imaging results are presented elsewhere, Garcia *et al.* (1992)]. Adjuvax[®] and BCG cells were chosen because they are important adjuvants, there are published electron microscopy studies of yeast wall derivatives and BCG and other mycobacteria, and because they have some unique properties that facilitate imaging. From the standpoint of scanning probe imaging, these biomaterials are easy to identify on substrates since they have distinct morphology and they are relatively large (micrometer-scale) structures. Also, sample preparation is simplified since BCG and the Adjuvax[®] particles are considered to be very hydrophobic, hence aqueous deposition onto a hydrophobic substrate such as graphite is possible. Finally, we believe that since these adjuvants are quite rigid when compared to other cells or membrane materials, image quality is improved by avoiding drastic deformation due to probe induced forces.

Materials and Methods

Sample preparation for BCG cells

For the STM experiments, BCG cells (Pasteur 1173) in Dubos medium at pH = 7.4 with 1% bovine serum albumin and 0.05% Tween-80 were provided by Ken Stover (MedImmune Inc., Bethesda, MD) and Vidal de la Cruz. The viable organisms were either heat killed at 70°C for 30 minutes or killed by addition of sodium azide. The STM experiments were performed in a liquid sample chamber with graphite (HOPG Grade ZYB) as the substrate. In the liquid sample chamber, the BCG cell concentrations was about 5×10^8 organisms/ml and the buffer solution was phosphate buffer (pH = 7.4) with 0.05% Tween-80.

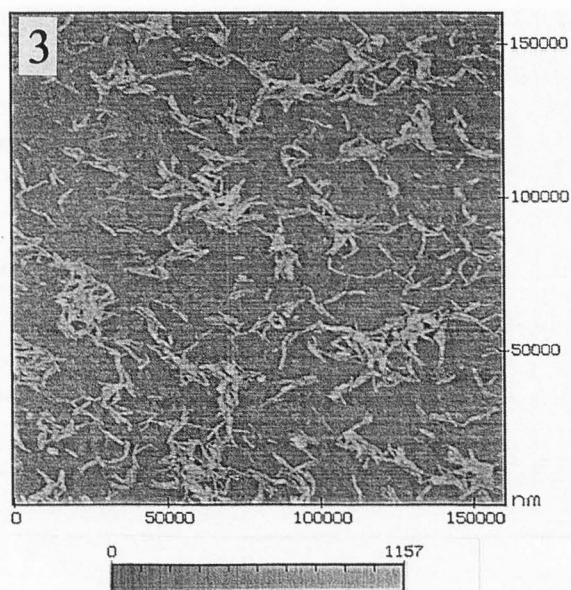


Figure 3. An AFM image of BCG immobilized on a glass slide. The units for x,y,z scales are nm. The z scale is shown as a grey bar to the right of the image. BCG cord formation is quite evident. The low contrast patches are believed to be either fragments of the cell membrane or extracellular microgranules (Kolbel, 1984).

For the AFM experiments, a solution with suspended, killed BCG were spun down onto a glass slide or a graphite (HOPG Grade ZYB) substrate using a Cytospin (Shandon Lipshaw Corp., Pittsburgh, PA). The culture was placed in a 2 ml (Falcon 2059) tube and mildly sonicated in a cup sonicator. After sonication, the culture was diluted to a BCG cell concentration just below the monolayer coverage for the deposition area on the glass slide or graphite substrate. After centrifugation, the cells were washed with methanol or formalin in order to remove weakly bound cells and to preserve the cells through dehydration.

Scanning tunneling microscopy

The scanning tunneling microscope used was based on a prototype designed at Arizona State University. A simple wet chemical cell (120 ml capacity) was fashioned by cutting a polypropylene microcentrifuge tube and placing it over the HOPG grade ZYB graphite (Union Carbide, Cleveland, OH) substrate after applying apiezon wax around the tube to prevent liquid leakage. To operate the STM in aqueous solutions, a platinum iridium tip coated with apiezon wax (Nagahara *et al.*, 1989) or an electrochemically etched tungsten tip coated with apiezon wax was used. Images of BCG cells were collected at various tip bias voltages and tunneling currents, although many images were obtained at -300 mV tip bias and a tunneling current between 0.2-0.5 nanoamperes (nA). A scanning head capable of a z-extension maximum range of 3100 nm and a maximum x-y scan range of 75 μm was used. All imaging data shown in

Figures 6-9 are unfiltered.

Atomic force microscopy

A Nanoscope II (Digital Instruments, Santa Barbara, CA) and an Ambient System AFM (Park Scientific Co., Sunnyvale, CA) were used for the AFM experiments. AFM experiments with BCG cells were performed on the dry, centrifuged cells. As with the STM experiments, HOPG Grade ZYB graphite was used as the substrate for some BCG AFM imaging. BCG cells immobilized on glass slides were also imaged. The Nanoscope experiments used a 200 μm thin leg cantilever with a silicon nitride tip (Digital Instruments, Santa Barbara, CA) and a piezo scan tube with a maximum x-y scan range of 160 μm . Experiments with the Park Scientific Ambient AFM were conducted with a 4.5 μm conical tip silicon cantilever (Park Scientific Co., Sunnyvale, CA) and a scan tube with a maximum x-y scan range of 250 μm and a maximum z-extension of 14 μm . The hard-core repulsive force curve was optimized so that about 2×10^{-9} Newtons of force was used during constant force mode scanning. Images were collected in the constant force mode. The imaging data shown in Figures 3-5 are unfiltered.

Optical and scanning electron microscopy

A Wild M-20 optical microscope was equipped with a Polaroid camera to obtain photographs of BCG cells on glass slides. A maximum magnification of 770x was achieved with this instrument. The same sample observed with the optical microscope was coated with aluminum and imaged with an ISI-100B scanning electron microscope (SEM).

Results and Discussion

The focus of this paper is to show that scanning probe microscopy can be used to obtain the detailed morphology of BCG cells by comparing AFM and STM imaging results with electron and light microscopy. Care was taken to obtain representative images by repeating the imaging experiments with different BCG samples. Since the mechanism for STM imaging of uncoated biomolecules is poorly understood and hotly debated, this study is meant to determine if cell surface images from STM are reproducible and if they compare with known morphology using other imaging techniques.

Mycobacteria are well known for their tendency to form cords consisting of multiple individual cells oriented in parallel due to hydrophobic interactions (Kolbel, 1984). Figure 1 is a photograph taken by light microscopy clearly illustrating cord formation as well as the cigar-shaped structure of single BCG cells which are about 2.5 to 3.5 μm in length and 0.6 μm in width (Darzins, 1958). Higher magnification, attainable by the scanning electron microscope, also shows cord formation (Figure 2). This sample was coated with aluminum in order to obtain a stable image.

Figure 3 shows a relatively large-scan area AFM image of another glass slide containing BCG cords and single cells. The centrifuged BCG is easily imaged in

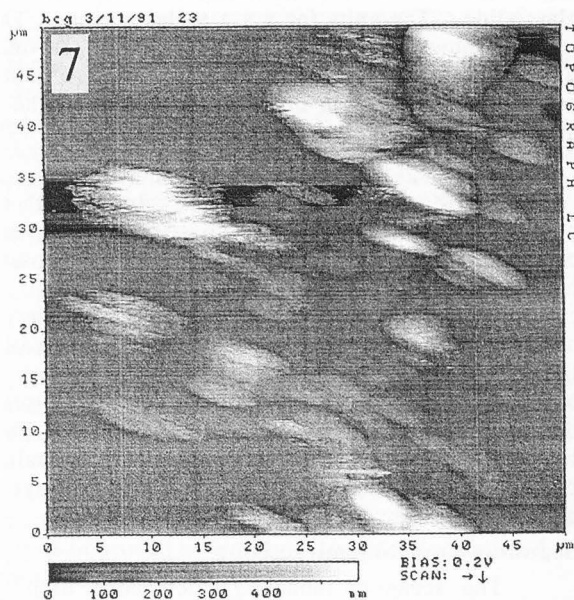
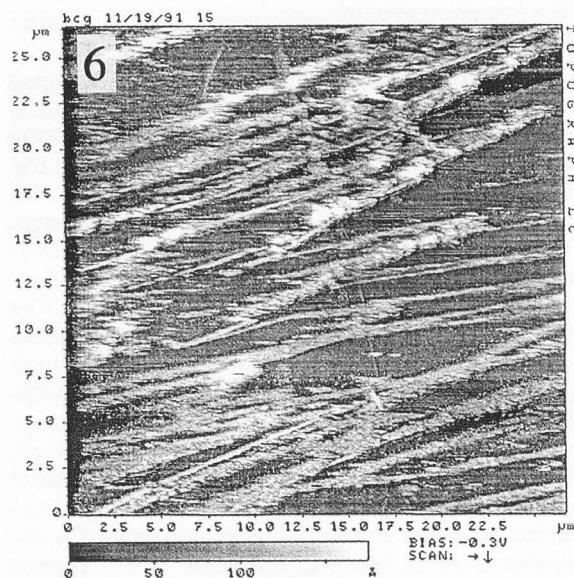
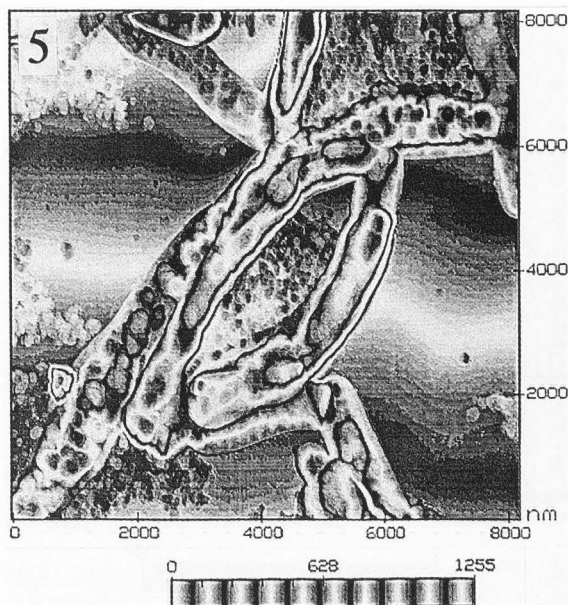
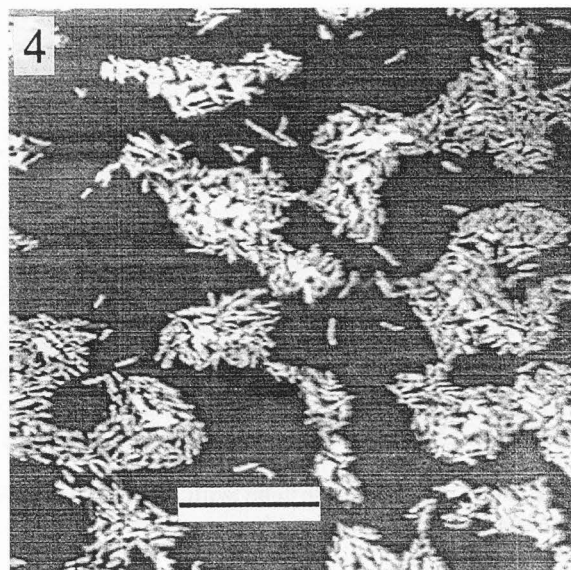


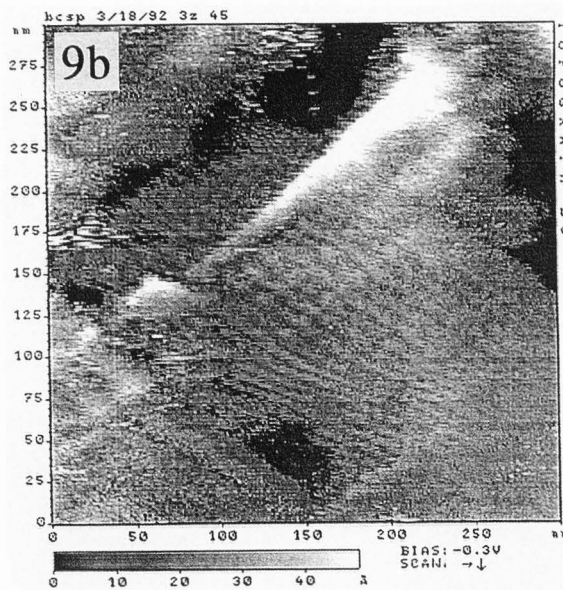
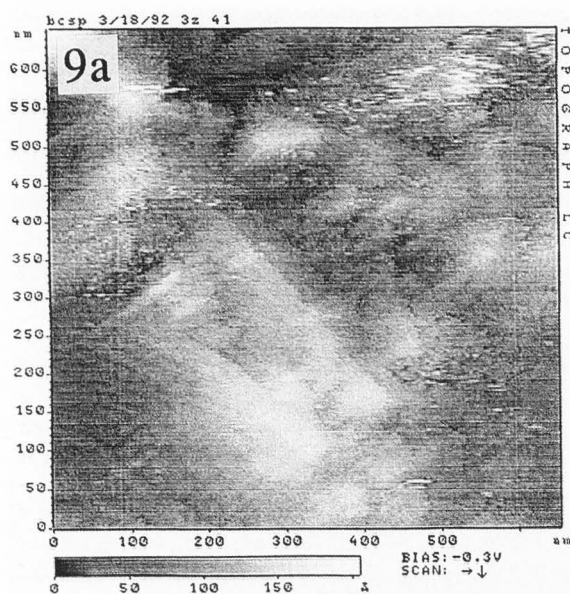
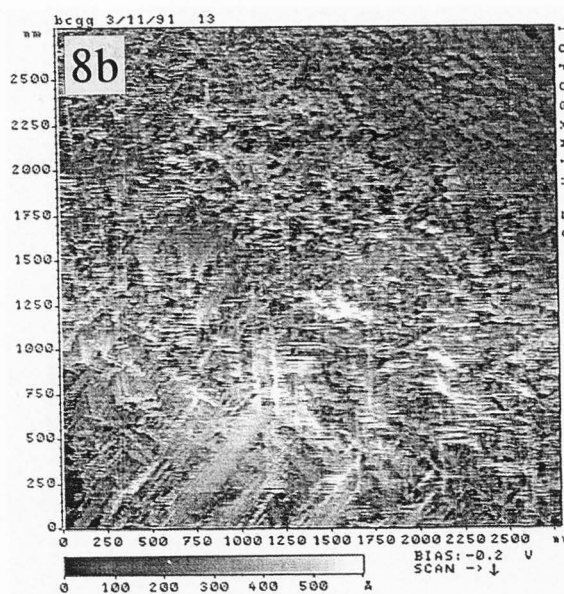
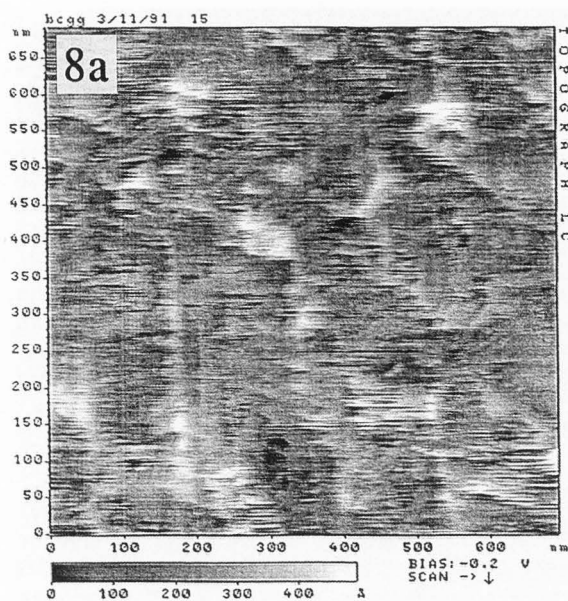
Figure 4. An AFM image in air of BCG immobilized on a graphite (HOPG grade ZYB) substrate. Extracellular material is not evident in this preparation. Bar = 50,000 nm.

Figure 5. A higher resolution AFM image of BCG of a section of the same sample area shown in Figure 3. Extracellular microgranules or cell membrane fragments surround the BCG. Varying BCG topography indicate regions which have similar structure to vacuoles or phosphate granules identified in electron microscopy (Kolbel, 1984). The grey scale was altered in order to highlight the AFM contrast information. All scales are in nm.

Figure 6. An STM image of BCG immobilized on graphite under aqueous solution. A graphite cleave plain is evident showing that the BCG is not oriented along the graphite defect. The contrast information, or "height", is much lower than the "height" by AFM.

Figure 7. Another STM image of BCG on graphite under aqueous solution. The image was generated using a different BCG sample than the one used to obtain the image in Figure 6. The contrast information is much higher than the data in Figure 6.

BCG cell imaging using scanning probe microscopy



air with the AFM. Samples prepared using glass slides (Figure 3) and graphite (Figure 4) give similar results. Figure 5 gives a more detailed image of an individual BCG cell showing distinct regions which may be due to vacuoles or phosphate granules (Darzins, 1958; Kolbel, 1984). Besides the overall confirmation of cord structure morphology by AFM imaging, we also noticed the presence of very small disk-like structures (see Figure 5) around the BCG cords for centrifuged samples stored several months prior to imaging. These structures were not evident in all of the BCG cell samples imaged with the AFM or in samples of *E. coli* cells prepared in the same fashion and stored for several months as well. The disk-like structures may be fragments of BCG cell walls (i.e., blebs) or, based on published electron microscopy

Figure 8. A sequence of STM images with successively higher resolution of a BCG cell under aqueous solution immobilized on a graphite substrate. The sample used is the same one used to obtain the image in Figure 7. The lower contrast regions are similar to electron microscopy results (Lounatmaa and Barnder, 1989).

Figure 9. Another two image sequence showing higher resolution STM images of a BCG cell under aqueous solution immobilized on a graphite substrate. The sample used for this image was the same one used to obtain the AFM image in Figure 4 and the STM image in Figure 6. A portion of the structure has a periodic layer which is characteristic of some regions of the outer cell surface of mycobacteria (Draper, 1982; Kolbel, 1984).

results (Kolbel, 1984), extracellular microgranules. These structures cannot be observed by optical microscopy.

For the BCG immobilized on graphite imaged in Figure 4, we were unable to get clear STM images of the centrifuged cords when imaging in air. The STM images obtained were extremely "streaky" and difficult to interpret. A number of likely factors contribute to the difficulty of STM imaging of BCG in air. From visual inspection of the STM probe after imaging in air, we noticed that there was an accumulation of material at the end of the probe. This observation indicates that the STM probe can remove BCG from the surface during imaging since the STM probe was not found to accumulate material at the tip when imaging bare graphite.

However, when BCG is imaged with the STM in aqueous solution, images shown in Figures 6 and 7 are obtained. Note that in Figure 6 a graphite step is evident, but it is oriented at a different angle than the BCG and in fact some of the cords span the cleave planes. The stability of BCG bound to the graphite surface under aqueous solution is thought to be partly due to water packing forces augmented by the hydrophobic effect. Eriksson *et al.* (1989) have developed a mean-field theory for describing hydrophobic attractive forces that predicts a rapidly increasing force at small separation distances. Their results agree well with measured hydrophobic forces of 10^{-5} N for surface separations less than 2 nm (Claesson *et al.*, 1987; Christenson and Claesson, 1988; Claesson and Christenson, 1988).

Another observation concerning Figures 6 and 7 is that the height or contrast of a BCG cell measured with the STM varies by an order of magnitude. Different samples and STM probes were used to obtain these images. STM images of yeast cell walls have also shown variable contrast with average heights being markedly lower than measured by AFM or laser light scattering (Garcia *et al.*, 1992). The discrepancy in cell thickness between Figures 6 and 7 is likely due to the STM probe penetrating and/or compressing the cell.

Although researchers have reported that STM contrast information is difficult to interpret, the STM has also provided morphological detail on BCG cells that is unattainable with the AFM. STM images of a BCG cell surface shown in Figure 8 reveal several dark regions which are interpreted as recessed areas. This morphology agrees well with BCG cell electron microscopy images (Lounatmaa and Brander, 1989). STM imaging of a different BCG sample (Figure 9) shows that this morphology is not uniform and that periodic layers with a spacing of 5-10 nm can be seen in some regions. Images of a periodic layer are consistent with electron microscopy results (Kolbel, 1984; Lounatmaa and Brander, 1989). The ultrastructure of a mycobacterial wall contains an outer mycoside layer (Draper, 1982) that is typified by a fibrillar morphology in which the strands of a particular mycoside network are in parallel.

Two contradictory observations from STM imaging of BCG cells can be summarized: (1) when the entire

cell is imaged the contrast is highly variable and usually lower than expected; and (2) however, when a scan of a part of the cell surface is performed, distinct and detailed features can be observed. If the probe penetrates the surface, as has been reported by other researchers (Ruppersberg *et al.*, 1989; Tang *et al.*, 1993), then the cell contrast will be lower and depend on the degree of penetration needed to establish a tunneling current. In this case the "surface features" imaged in Figures 8 and/or 9 would then actually relate to features beneath the top cell wall layer. Another possible explanation for the images in Figures 8 and 9 is that a non-tunneling mechanism (Tang *et al.*, 1993) was involved and that these images represent the topography of BCG cell surfaces.

Conclusions

AFM images show cord structure as well as variations in surface topography due to either vacuole or phosphate granule formation. AFM imaging of BCG cells can also reveal the presence of small extracellular structures which cannot be seen with the optical microscope. The STM can provide greater detail of the cell yielding images of periodic layers and other features; however, the height or contrast information is not easily interpretable. Fixation of the cells for imaging purposes can be accomplished either by utilizing the hydrophobic nature of the outer cell wall and allowing the cells to bind to a graphite surface from aqueous solution or by the action of centrifuging the cell suspension onto a substrate. Morphological features of BCG cells from optical and electron microscopy agree well with features imaged with both the STM and the AFM.

Acknowledgements

We are deeply indebted to Vidal de la Cruz for suggesting this work. We also thank him and Ken Stover for preparing the BCG cell samples. Funding for this work was provided by the National Science Foundation (BCS-90-09301 and DIR 89-20053), the Office of Naval Research (N00014-90-J-1455), the Whitaker Foundation and the Office of the Vice-President for Research at Arizona State University.

References

- Blackford BL, Watanabe MO, Dahn DC, Jericho MH, Southam G, Beveridge TJ (1989) The imaging of a complete biological structure with the scanning tunneling microscope. *Ultramicroscopy* **27**, 427-432.
- Butt HJ, Wolff EK, Gould SAC, Dixon Northern B, Peterson CM, Hansma PK (1990) Imaging cells with the atomic force microscope. *J. Struct. Bio.* **105**, 54-61.
- Christenson HK, Claesson PM (1988) Cavitation and the interaction between macroscopic hydrophobic surfaces. *Science* **239**, 390-392.
- Claesson PM, Blom CE, Herder PC, Ninham BW (1987) Interactions between water-stable hydrophobic Langmuir-Blodgett monolayers on silica. *J. Coll. Inter. Sci.* **114**, 234-242.

- Claesson PM, Christenson HK (1988) Very long range attractive forces between uncharged hydrocarbon and fluorocarbon surfaces in water. *J. Phys. Chem.* **92**, 1650-1655.
- Darzins E (1958) *The Bacteriology of Tuberculosis*. University of Minnesota Press, Minneapolis, 38-39.
- Draper P (1982) The anatomy of mycobacteria. In: *The Biology of the Mycobacteria*. Vol. 1. Ratledge C, Stanford J (eds.). Academic Press, London, 9-52.
- Eriksson JC, Ljunggren S, Claesson PM (1989) A phenomenological theory of long-range hydrophobic attraction forces based on a square-gradient variational approach. *J. Chem. Soc. Far. Trans. II* **85**, 163-176.
- Garcia AA, Oden P, Knipping U, Ostroff G, Druyer R (1992) Characterization of a β -glucan particle using scanning tunneling and atomic force microscopes. In: *Synthetic Microstructures in Biological Research*. Schnur JM, Peckerar M (eds.). Plenum Press, New York, 131-144.
- Gould SAC, Drake B, Prater CB, Weisenhorn AL, Manne S, Hansma HG, Hansma PK, Massie J, Longmire M, Elings V, Dixon Northern B, Mukergee B, Peterson CM, Stoeckenius W, Albrecht TR, Quate CF (1990) From atoms to integrated circuit chips, blood cells, and bacteria with the atomic force microscope. *J. Vac. Sci. Technol.* **A8**, 369-373.
- Haberle W, Hörber JKH, Binnig G (1991) Force microscopy on living cells. *J. Vac. Sci. Technol.* **B9**, 1211-1213.
- Henderson E, Haydon PG, Sakaguchi DS (1992) Actin filament dynamics in living glial cells imaged by atomic force microscopy. *Science* **257**, 1944-1946.
- Hörber JKH, Lang CA, Hansch TW, Heckl WM, Mohwald H (1988) Scanning tunneling microscopy of lipid films and embedded biomolecules. *Chem. Phys. Lett.* **145**, 151-158.
- Hörber JKH, Haberle W, Ohnesorge F, Binnig G, Liebich HG, Czerny CP, Mahnel H, Mayr A (1992) Investigation of living cells in the nanometer regime with the scanning force microscope. *Scanning Microsc* **6**, 919-930.
- Ito E, Takahashi T, Hama K, Yoshioka T, Mizutani W, Shimizu H, Ono M (1991) An approach to imaging of living cells' surface topography by scanning tunneling microscopy. *Biochem. Biophys. Res. Comm.* **177**, 636-643.
- Jericho MH, Blackford BL, Dahn DC, Frane C, and MacLean D (1989) Scanning tunneling microscope imaging of uncoated biological material. *J. Vac. Sci. Technol.* **A8**, 661-666.
- Kasa S, Gotzos V, Celio MR (1993) Observation of living cells using the atomic force microscope. *Biophys. J.* **64**, 539-544.
- Kolbel HK (1984) *Electron Microscopy*. In: *The Mycobacteria: A Source Book*. Volume 1. Kubica GP, Wayne LG (eds.). Marcel Dekker, New York, 249-300.
- Lounatmaa K, Brander E (1989) Crystalline cell surface layer of mycobacterium bovis BCG. *J. Bacteriol.* **171**, 5756-5758.
- Nagahara LA, Thundat T, Lindsay SL (1989) Preparation and characterization of STM tips for electrochemical studies. *Rev. Sci. Instrum.* **60**, 3128-3130.
- Putnam CAJ, de Grooth BG, Hansma PK, van Hulst NF, Greve J (1993) Immunogold labels: Cell-surface markers in atomic force microscopy. *Ultramicroscopy* **48**, 177-182.
- Ruppersberg JP, Hörber H, Gerber C, Binnig G (1989) Imaging of cell membranes and cytoskeletal structures with a scanning tunneling microscope. *FEBS Lett.* **257**, 460-464.
- Smith DW (1984) BCG. In: *The Mycobacteria: A Source Book*. Volume 2. Kubica GP, Wayne LG (eds.). Marcel Dekker, New York, 1057-1069.
- Stewart-Tull DES (1983) Immunologically important constituents of mycobacteria: Adjuvants. In: *The Biology of the Mycobacteria*. Volume 2. Ratledge C, Stanford J (eds.). Academic Press, London, 3-84.
- Stover CK, de la Cruz VF, Fuerst TR, Burlein JE, Benson LA, Bennett LT, Bansal GP, Young JF, Lee MH, Hatfull GF, Snapper SB, Barletta RG, Jacobs WR, Bloom BR (1991) New use of BCG for recombinant vaccines. *Nature* **351**, 456-460.
- Tang SL, McGhie AJ, Suna A (1993) Molecular-resolution imaging of insulating macromolecules with the scanning tunneling microscope via a nontunneling, electric-field-induced mechanism. *Physical Review B* **47**, 3850-3856.

Discussion with Reviewers

H.J. Butt: Figures 6 and 7 are supposed to show two samples of BCG cells prepared in the same way. The images are however totally different. Note for instance the height scale which is 170 Angstroms (17 nm) in Figure 6 and 550 nm in Figure 7. Why is this so? Which image is typical? Also, the details obtained on those samples (shown in Figures 8 and 9) are totally different. The conclusion of the paper that hydrophobic, rigid biological structures can be reproducibly imaged without metal coating was already reached by other authors (e.g., Hörber *et al.*, 1988; Blackford *et al.*, 1989; Ruppersberg *et al.*, 1989; Jericho *et al.*, 1990).

Authors: Height variation in STM imaging of biological materials has been widely reported. The most probable cause of height variation in imaging cells or cell wall ghosts is due to penetration of the material by the STM probe as pointed out by several investigators (Tang *et al.*, 1993; Ruppersberg *et al.*, 1989). Previous work on yeast cell wall ghosts (Garcia *et al.*, 1992) showed that STM heights are usually lower than heights measured by AFM and light scattering. BCG cell membranes are made up of several layers with quite different morphologies (Draper, 1982). One possible explanation for the differences between Figures 8 and 9 is that the STM tip is penetrating the membrane and imaging different membrane layers. For BCG cells, a typical height should be approximately 500 nm.

H.J. Butt: Were all cells shown in the paper treated with methanol or only those imaged with the AFM? If this is the case, the structure of the cells might not have much in common with the native cells. Were the cells fixed before treating them with methanol?

Authors: Only cells prepared for AFM imaging were treated with methanol or formalin. The cells were spun down onto a graphite substrate or a glass slide before applying the organic solvent. Comparing our LM, EM and AFM images with LM and EM work by other researchers we do not see any differences in cell structure. We conclude that our immobilization technique does not induce any more structural changes than techniques used by other investigators.

J.K.H. Hörber: I tried STM imaging of cells some years ago and my experience is that it is very difficult to assure that the STM tip stays on top of the cells. In most cases, it was more reasonable to assume that the cell was actually penetrated by the tip, which, therefore, rather scanned the well fixed cell membrane in direct contact with the HOPG. Figure 9 looks very similar to what we saw in those experiments (Ruppersberg *et al.*, 1989).

Authors: We agree that STM tip penetration occurs frequently when imaging cells. However, in some cases heights obtained by STM imaging compare well with the expected values (see Figure 7). We are not certain how far the STM tip penetrated the cell when scans were limited to a section of the cell. In any event, the STM can obtain molecular resolution images of uncoated large biological structures (Tang, *et al.* 1993).

J.K.H. Hörber: The resolution of the AFM of biological samples can be much higher than the authors state in their conclusions. We got resolutions down to about 10 nm of living cells (Haberle *et al.*, 1991), and resolutions of down to about 2 nm have been reported of bacterial HPI- and S-layers.

Authors: AFM resolution from sample to sample will differ because AFM image resolution depends in part on the coupled effects or phenomena of contact force and sample rigidity, as well as probe aspect ratio and sample roughness. We may improve our resolution by using sharper probes or by using tapping or non-contact AFM modes.

K. Lounatmaa: What type of periodicity was detected in the outermost part of the cell wall? Have the authors tested the periodicity (Figure 9) using e.g., crystallographic methods?

Authors: The periodicity shown in Figure 9 manifests itself by alternating regions of higher and lower contrast which form parallel bands. The bands are not rectangular. In regions where kinks appear, the bands appear compressed. We did not test the periodicity with any other method.

K. Lounatmaa: The outermost layer of the cell wall of many bacteria, also mycobacteria, easily disappears during many cultivation steps. Have the authors assured of the existence of this layer on the cells studied?

Authors: We cannot assure the existence of the outer cell wall layer since a chemical analysis of the BCG cell wall for the samples used in this study was not done. We did minimize passage of BCG after cracking vials of freeze-dried Pasteur 1173 A2 reference strain, but we have no way of knowing if the cell wall on cultured BCG is like the cell wall of *in vivo* BCG.